Available online at www.sciencedirect.com
ScienceDirect
International Journal of Heat and Fluid Flow 28 (2007) 28–36
International Journal of HEAT AND FLUID FLOW
www.elsevier.com/locate/ijhff

Experimental study on compressible flow in microtubes

G.P. Celata [a,*], M. Cumo [b], S.J. McPhail [a], L. Tesfagabir [a], G. Zummo [a]

[a] *ENEA, Institute of Thermal Fluid Dynamics, Via Anguillarese 301, 00060 S.M. Galeria, Rome, Italy*
[b] *University of Rome La Sapienza, Corso Vittorio Emanuele II, 244 Rome, Italy*

Accepted 27 April 2006
Available online 9 August 2006

Abstract

Gas flow in microchannels has practical advantages compared to the use of liquids, in that system requirements are generally of a lighter and less fragile nature. However, the aspect of compressibility becomes an issue to take into account. Due to the high frictional head loss in microscopic channels, gas density can vary up to an order of magnitude between inlet and outlet, and correspondingly alter the shape and magnitude of the velocity profile. In this article the possible effects of this microscale phenomenon are investigated. To this effect, an experimental procedure for determining a local friction factor is implemented, and compared with a linearized global friction factor. Furthermore, a quantitative comparison between the linearized (incompressible) approximation and two ''quasi-compressible'' correlations for the friction factor is included.

The results show a remarkably accurate prediction of the friction factor by the reference curve of Hagen-Poiseuille, $f = 64/Re$, regarding the global as well as the local approximations, and a very close agreement between the incompressible and quasi-compressible correlations. This goes to indicate that the afore-mentioned effects of density-change-induced acceleration are extremely limited on a practical scale, and that an incompressible characterization is valid within the studied conditions of flow. The range of validity is synthesized in a limiting value of the pressure ratio at a given experimental uncertainty.

Keywords: Gas flow; Microtube; Experimental; Friction factor; Fused silica pipe; Poiseuille number

1. Introduction

The miniaturization of many appliances in biomedic, chemical and computer technology has brought with it increased demands for space-efficient high-performance heat dissipation and catalytic devices. Though much research on microscale level has already been done in recent years in the relevant fields, especially as regards hydrodynamic and heat transfer characterization, there is still much diversion of results to be discerned in the various experimental and numerical reports. The main difficulty in this new dimension of applied physics is the reliability of measurements, as conventional measuring apparatus is simply too big or coarse to implement in the tested system. As progress is being made, however, the tendency is for published results to be more orderly, and to converge towards the classical theories more than was originally expected.

Conditions are fairly extreme and difficult to control at microscale, but in the case of microchannel gas flow, there is a major advantage over liquid flow in the distinctly lighter system requirements. Pressures do not achieve extreme values and no pumping equipment is strictly necessary. On the other hand, compressibility of the fluid becomes an issue, as also molecular rarefaction.

For flow in microtubes, there are several theoretical studies dealing with the effect of the compressibility on gas flow. Van der Berg et al. (1993a,b) and Choquette et al. (1996) solved the isothermal, compressible Navier–Stokes equations for laminar flow in a circular tube. For low Reynolds number and Mach number flows the former obtained a local ''self-similar'' velocity profile with the product fRe still equal to 64. Beskok et al. (1996) numerically modelled the

* Corresponding author.
E-mail address: celata@casaccia.enea.it (G.P. Celata).

0142-727X/$ - see front matter © 2006 Elsevier Inc. All rights reserved.
doi:10.1016/j.ijheatfluidflow.2006.04.009

Nomenclature

c	speed of sound, m/s
D	channel diameter, m
e_y	absolute error of parameter y
F	force, N
f	Darcy friction factor, –
G	mass flux per unit area, kg/m^2 s
Kn	Knudsen number, λ/D
L	channel length, m
Ma	Mach number, U/c
P	measured pressure, Pa
p	pressure variable, Pa
Po	Poiseuille number, fRe
R	specific universal gas constant, J/kg K
r	radius variable, m
Re	Reynolds number, $\rho UD/\mu = 4\Gamma/\pi\mu D$
R_P	pressure ratio, P_{in}/P_{out}
T	temperature, K
u	fluid velocity variable, m/s
U	bulk fluid velocity, m/s
x	axis position variable, m

Greek symbols

α	channel cross-section geometrical coefficient
Γ	mass flow, kg/s
γ	ratio of specific heats
λ	molecular mean free path, m
μ	dynamic viscosity, Pa s
ρ	fluid density, kg/m^3
σ_v	momentum-accommodation coefficient
τ	tangential stress, N/m^2
σ	slip-flow friction factor correction term
Ω	perimeter, m

Subscripts

cont	pertains to continuum flow
f	pertains to friction or the friction factor
in	inlet
out	outlet
slip	pertains to slip flow
w	pertains to channel wall

competing effects of compressibility and rarefaction in internal flows in long channels. For shear-driven flows, the rarefaction dominated the momentum and energy transport, and the compressibility was negligible. Guo and Wu (1997, 1998) found that the gas density variation in the flow direction might be very large if the surface friction induced pressure drop per tube length was much larger than for conventional size tubes. Numerical solution of the governing equations for compressible flow in a circular tube led them to conclude that the continuous variation in shape of the velocity profile along the channel means that no fully developed and no locally fully developed flow will occur. On the other hand, Harley et al. (1995) conducting an experimental and numerical investigation of sub-sonic, compressible flow in similar, long conduits, suggested that the locally fully developed approximation could be used to interpret the experimental data for low and moderate Mach number flow.

Kohl et al. (2005) did a numerical and experimental study on compressible (air) flow with internal pressure measurements in the microchannel. They considered adiabatic governing equations in their model and found good agreement between the predicted and measured local pressures, but did not quantify the compressibility effects noted, apart from stating that these might increase the critical Reynolds number above 2300. This in contrast with earlier observations, reported in their work, that declared transition to turbulence to be anticipated, at Reynolds numbers as low as 350. Turner et al. (2004) also did experiments with internal pressure measurements, and investigated the effects of Mach and Knudsen numbers and of surface roughness. Using the isothermal characterization as a reference, they noticed an increase in local friction factor only at the channel inlet, and a decrease at rarefaction levels of $Kn > 0.01$. The influence of compressibility was also mapped, but, imprecisely, related to Mach number only. As is stated in Perry's Chemical Engineer's Handbook (Perry and Green, 1999): "A common error is to assume that compressibility effects are always negligible when the Mach number is small. The proper assessment of whether compressibility is important should be based on relative density changes, not on Mach number."

A similar imperfection was committed by Asako et al. (2005), who, in a numerical and experimental study, found a dependence of the friction factor on Mach number. Their experimental set-up and methodology, however, were exceedingly precise and intelligently prepared, and the numerical simulation was qualitatively confirmed. Only high Reynolds (>1500) and Mach number (>0.15) flows were investigated though.

Morini et al. (2004) presented a very useful work on the experimental validation of slip-flow models, working out the detectability of rarefaction effects given certain experimental uncertainties, and a quantification of these for various cross-sectional shapes. They did consider, however, only gas flow at extremely low pressure ratios, thus maintaining near-incompressible conditions.

This study aims to unite some of the aspects of the works cited, trying first of all to explain the particular importance of compressibility in microchannels, and then to give a practical context of its effects. Thus, two hydrodynamic models for compressible flow (isothermal and adiabatic) are confronted at normal conditions, and an experimental approximation of a local friction factor is devised to compare with the global friction factor and

thereby quantify the effect of compressibility. There is also a brief mention of rarefaction detectability, taken from Morini et al. (2004).

2. Friction factor for non-linear head loss

Frictional force in laminar flow is caused by tangential deformation of the fluid through interaction with the channel wall. To solve the set of conservation equations (i.e. equations of continuity, momentum and energy) which govern one-dimensional compressible flow through a constant-area channel – in particular, the momentum equation – it is necessary to express the wall shear stress τ_w in terms of flow variables along the axial distance, x, through the channel. For a control volume in such a duct, the frictional force (dF_f) is expressed as

$$dF_f = \tau_w \Omega \, dx \tag{1}$$

where Ω is the wetted perimeter.

The high-pressure drops involved in microscopic flow cause, in the case of gas being the working fluid, large variations of density in the duct even at *low speeds* ($Ma < 0.3$). The change in density as the gas loses pressure causes a change of the fluid bulk velocity, and thus also of the velocity profile. This means that the expression for τ_w in the defining equation of the dynamic viscosity for Newtonian fluids, μ,

$$\tau_w = \mu \frac{\partial u(x,r)}{\partial r} \tag{2}$$

is no longer explicit because of the dependence of the velocity $u(x,r)$ on x (assuming μ constant). We obtain a statically indeterminate set of defining (conservation) equations where we are trying to determine the crucial, independent variable F_f.

For *incompressible* flow (where the velocity profile is known and the head loss along the channel axis is linear), τ_w can be written in terms of flow properties and the friction factor, f:

$$\tau_w = \frac{f \rho U^2}{8} \tag{3}$$

This leads, for laminar flow, to the well-known correlation of Hagen-Poiseuille, which states that the product between the friction factor f and the Reynolds number Re is a constant. For circular tubes, this constant (the Poiseuille number Po) is 64.

To solve the indeterminate set of conservation equations, in the literature Eq. (3) is adopted to describe also the case of *compressible* flow. This is assumed to be valid where sub-sonic velocities are concerned. An assumption, however, which is based on experience with conventionally sized pipes, where frictional pressure drop is almost negligible for low-viscosity gas flow. The equations of continuity and energy however, can then take compressibility into account, so that the solution of the indeterminate problem amalgamates physically sound conclusions with an approximation which was intended originally for different conditions.

In this study we aim to compare a linearized, local friction factor measured experimentally, with a global friction factor taking into account the entire length of channel, in order to determine the magnitude of the compressibility effect. Also, these friction factors are compared with those obtained from correlations derived from the assumption of Eq. (3). These correlations are the following.

For *isothermal* flow in a circular duct with diameter D, the description of the friction factor obtained becomes (Choquette et al., 1996):

$$f \frac{\Delta L}{D} = \frac{p_{in}^2 - p_{out}^2}{RTG^2} - 2 \ln \left(\frac{p_{in}}{p_{out}} \right) \tag{4}$$

For frictional *adiabatic* (Fanno line) flow, the temperature term is added to the equation of state for an ideal gas:

$$\frac{dp}{p} = \frac{d\rho}{\rho} + \frac{dT}{T} \tag{5}$$

which leads to the following expression for f (Kohl et al., 2005; Fox and McDonald, 1994):

$$f \frac{\Delta L}{D} = \frac{p_{in}^2}{RT_{in}G^2} \left(1 - \frac{p_{out}^2 T_{in}}{p_{in}^2 T_{out}} \right) + \frac{\gamma + 1}{2\gamma} \times \ln \left(\frac{T_{in}}{T_{out}} \cdot \frac{2p_{out}^2 \gamma + (\gamma - 1) R T_{out} G^2}{2p_{in}^2 \gamma + (\gamma - 1) R T_{in} G^2} \right) \tag{6}$$

In these equations, the pressures p_{in} and p_{out} represent the net values at inlet and outlet of the channel section ΔL along which the *average* friction factor is sought. G is the mass flux per unit area, γ the proportion of specific heats, R the (specific) universal gas constant.

In the next paragraph, the methodology of the experimental approximation is set out that was used to determine f, in order for the comparison to take place.

3. Experimental procedure

3.1. Determining a local friction factor for non-linear head loss

An experimental verification of a net, local friction factor was attempted by executing fluid-dynamic measurements for two lengths of tube of identical diameter. At equal mass flow rates, the longer tube must have a higher frictional pressure drop than the shorter one, but concentrated pressure losses (inlet and outlet effects) should be the same. From this assumption a *net* frictional head loss can be deduced (Celata et al., 2006).

This method is well proved for incompressible flows, where the pressure drop is linear along the channel; for flows with changing density its applicability needs to be justified.

Qualitatively, the head loss along a microchannel for a compressible fluid is as schematised in Fig. 1 (Guo and Wu, 1997; Ettre and Hinshaw, 1993).

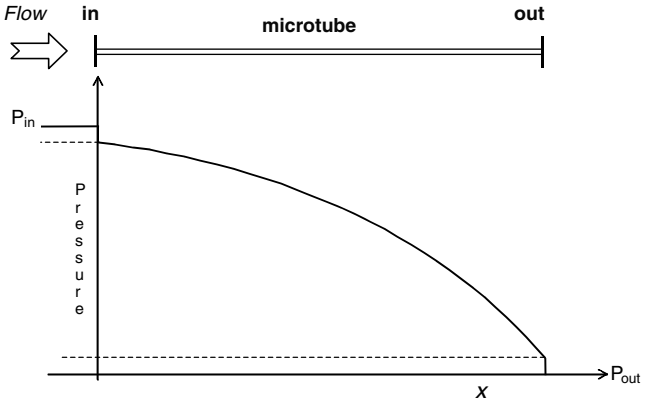

Fig. 1. Schematization of head loss along a microchannel for a compressible fluid.

The difference between the *measured* values of the pressures at the inlet (P_{in}) and outlet (P_{out}) of the tube does not correspond to the *actual* frictional head loss (between the dashed lines) because they contain concentrated losses due to geometry effects (contractions, expansions, flow separation, etc.) at the test section fittings. The same mass flow passing through a *shorter* tube with the same exit pressure (ambient) will have an identical profile to the one in Fig. 1 – they overlap in other words – from the outlet backwards, with the inlet step occurring at a lower pressure than P_{in}. Assuming this step – which represents a concentration of all inlet effects – of the same size as for the long tube (which is acceptable for a relatively short ΔL), subtraction of the two measured *gross* pressure differences will yield the *net* frictional head loss in the high-pressure section of the long tube (see Fig. 2).

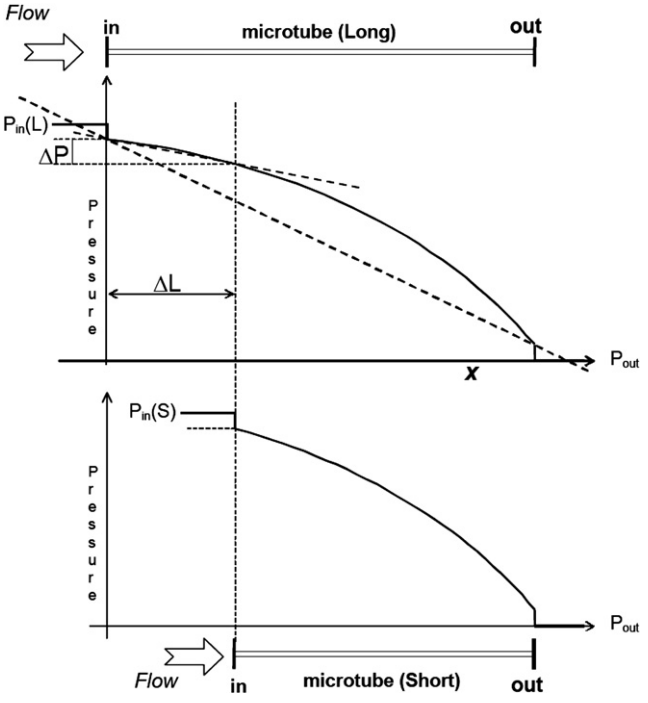

Fig. 2. Pressure profile along different lengths of microtube.

The friction factor being equivalent to the slope of the pressure profile, an experimental approximation should be more accurate with the above method than by considering one length of tube alone, as the tangential (dashed) lines in Fig. 2 indicate. Increasing the length of tube to diminish the weight of the concentrated losses on the total pressure drop would not improve precision because the non-linearity of the head loss would be more accentuated. The experimental (linearized) friction factor is taken directly from the Darcy equation, and is calculated as follows:

$$f\frac{\Delta L}{D}=\frac{\pi^2\rho\Delta P D^4}{8\Gamma^2} \tag{7}$$

where ΔP and ΔL are as defined in Fig. 2 for the *differential* friction factor calculation. We shall refer to this also as the *local* friction factor, so that it is clear that this value depends on the various flow parameters as well as the axial position. For the global friction factor (taken over the entire length of the *longer* tube) respectively the difference between $P_{in}(L)$ and P_{out} is used and the length of the entire long tube, L. ρ is the density at the linear average pressure in the section of tube under consideration (ΔL or L), and γ is the measured mass flow.

3.2. Overview of experiments

In this study we aim to evaluate the degree of non-linearity of the pressure drop in a microchannel, or how big the difference is between the local friction factor and the average global friction factor (taken over the entire length of the longer tube) as illustrated in Fig. 2. Also a comparison with the "quasi-compressible" definitions of the friction factor in Eqs. (4) and (6) is effectuated. The incompressible definition of the friction factor $f = 64/Re$, will thereby serve as reference.

The tubes tested are reported in Table 1. From the column of the pressure ratios it can be seen that it cannot be justified to consider the flow incompressible, because for an ideal gas the density is linearly dependent on the pressure. This means that in a 50 μm tube the difference in density can amount to an order of magnitude between inlet and outlet, with the Mach number correspondingly increasing from 0.02 to 0.2 – that is, remaining below the limiting value of 0.3 usually adopted for valid incompressible approximation.

The measurements of the tube diameters are made with a Gemini Scanning Electron Microscope (LEO 1530). A

Table 1
Channels under consideration

Diameter (μm)	e_D (μm)	L/D	Pressure ratio	Reynolds	Knudsen $\times 10^3$
254	8.2	300–360	1.1–2.2	30–500	0.4–0.8
101	2.5	600–850	1.1–5.0	5–250	0.4–1.9
50	1.6	1000–1250	2.4–9.2	5–100	0.5–4.7
30	1.1	1800–2400	2.2–10	0.8–13	0.3–6.4

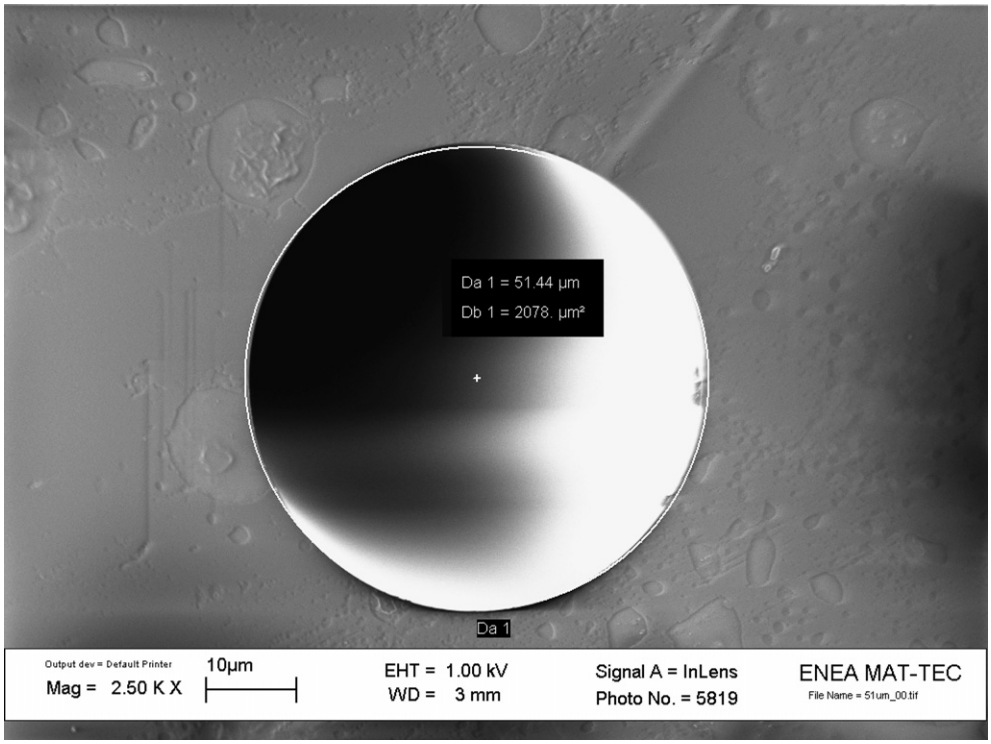

Fig. 3. SEM image of a cross-section of the 50 µm tube.

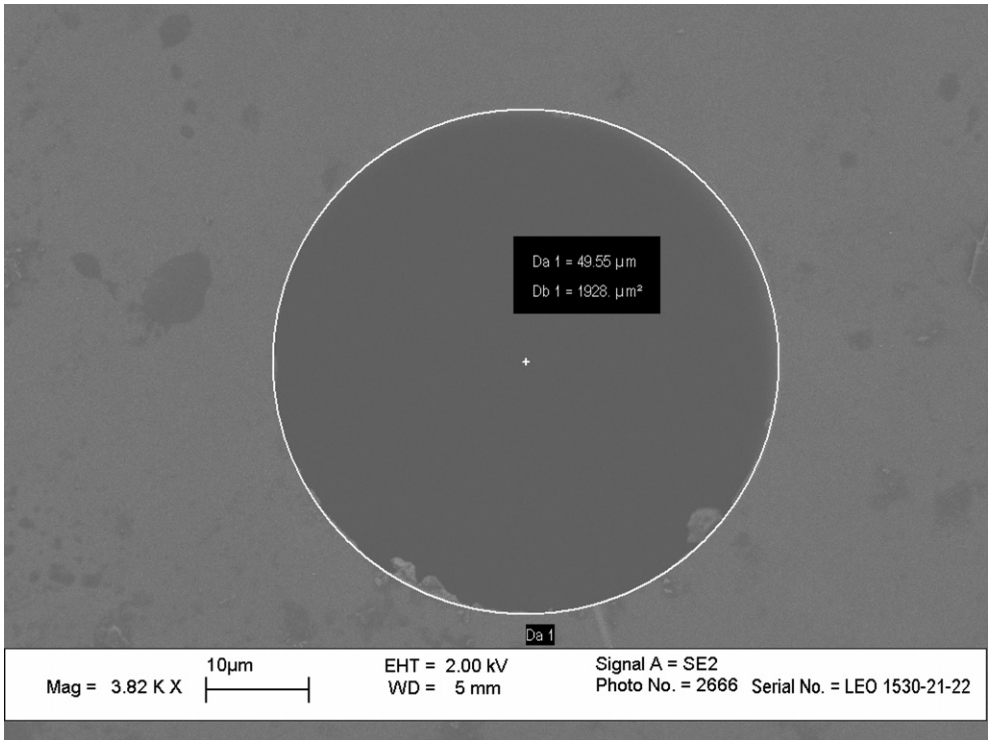

Fig. 4. SEM image of a different cross-section of same tube.

circle is projected over the image and the diameter is taken of the best fit of the channel circumference (see Figs. 3 and 4). The uncertainty on the average value is mainly due to non-perfect circularity or slight axial variations of the channel geometry, as is evident from comparing Figs. 3 and 4, which are two different cross-sections of the same capillary tubing.

The absolute roughness of the tubes is less than 0.05 µm. The length-to-diameter ratios in Table 1 are indicative of the two lengths of test sections, cut from the same capillary to

ensure similarity between the two inside surface conditions. Although in compressible conditions one cannot speak of fully developed flow at any stage of the flow due to the constantly changing, density-based velocity profile, the lengths in Table 1 are considered to be such as to minimize disturbing effects such as flow separation and turbulence due to the sudden geometry changes at the inlet and outlet.

3.3. Influence of slip flow

At small diameters, rarefaction of the gas becomes an issue. This is especially the case at low pressures (channel outlet) where the mean free molecular path λ approaches the dimensions of the channel. This is expressed in the Knudsen number:

$$Kn = \frac{\lambda}{D} \tag{8}$$

Fully rarefied flow is assumed to occur from Kn values that are higher than 10, but already at $Kn = 10^{-3}$ effects are supposed to be visible (slip flow). As opposed to continuum flow, in rarefied conditions there is no bulk viscosity as such present in the fluid and the assumptions on which the Navier–Stokes equations of motion are based are no longer valid. In the limiting case where there is just fluid slip at the wall however, the effects are merely of a reduced head loss and a correction on the (continuum) friction factor is usefully adopted:

$$f_{\text{slip}} = \Phi \cdot f_{\text{cont}} \tag{9}$$

This is called the first-order slip model, and the correction term σ is expressed in terms of a geometrical coefficient α. In case of uniformly diffusive surfaces (i.e. the momentum-accommodation coefficient σ_v is equal to unity):

$$\Phi = \frac{1}{1 + \alpha Kn_{\text{slip}}} \tag{10}$$

In Morini et al. (2004) this correction term is explained, and various values of it are reported for several channel cross-sections. For a circular geometry, α is equal to 8. The implication of this in experimental investigations is related particularly to the experimental accuracy. In Morini et al. (2004) it is thus shown that for a given Reynolds number, the effect of gas rarefaction cannot be evidenced if

$$f_{\text{slip}}(1 + U_f) \geqslant f_{\text{cont}} \tag{11}$$

where U_f is the total experimental uncertainty. This means that the lowest Knudsen number for which it is possible to experimentally pinpoint effects on the friction factor due to rarefaction is

$$Kn_{\min} = \frac{U_f}{\alpha} \tag{12}$$

The experimental uncertainty of the test rig, U_f, depends on its constituent components.

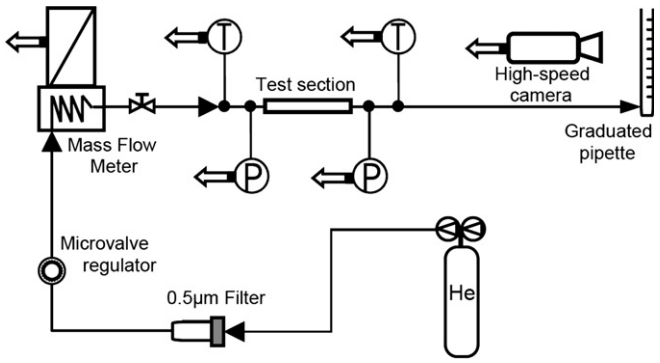

Fig. 5. Schematic of the experimental test-loop.

3.4. Experimental set-up

A scheme of the test rig is presented in Fig. 5. The working fluid is helium, which is supplied to the test loop by a pressurized cylinder. The flow is controlled through a two-stage pressure reduction regulator and is relieved of particulate matter through a 0.5 μm filter. The fine-tuning of the inlet pressure is done with a microvalve regulator. Pressure measurements are made just before the inlet and just after the outlet of the test section by absolute pressure transducers (Druck PTX100/IS, 0–35 bar) and in parallel by a differential manometer (Rosemount 1151DP, 0–6.85 bar). The open arrows in the figure indicate data acquisition (PC AT-MIO-16XE-50 acquisition board, LabView 6i acquisition programmes).

The capillaries tested are fused silica tubes, mounted with high-pressure, near-zero dead volume gas chromatography fittings (Upchurch Scientific). For measuring the mass flow, two methods were applied. At relatively high mass flow rates ($\Gamma > 5$ mg/min) the helium was passed through a pipette of known diameter carrying up with it a thin film of soapy water. The velocity at which the meniscus travelled through the pipette was recorded with a high-speed camera (SpeedCam+512) and elaborated from measured volumetric flow to mass flow. This is a simple and reliable method for gas flow measurement, but in the experimental error analysis the precision of the pipette diameter weighs almost as heavily as the test section diameter – see the following section on uncertainty analysis. For smaller mass fluxes, this method yielded unpredictable, scattered results. Therefore, a dedicated, high-precision thermal mass flow meter (Bronkhorst EL-Flow, 0–5 ml/min) was implemented for the experiments on the two smallest diameters. The gas is then expelled to the open air.

3.5. Uncertainty analysis

According to the classical methods described before by us (Celata, 2004), the experimental uncertainty of an investigated parameter – in this case the friction factor – can be described by

$$U_f = \frac{e_f}{f} = \sqrt{\left(\frac{5\,e_D}{D}\right)^2 + \left(\frac{e_{\Delta L}}{\Delta L}\right)^2 + \left(\frac{e_{\Delta P}}{\Delta P}\right)^2 + \left(\frac{e_\rho}{\rho}\right)^2 + \left(\frac{2e_\Gamma}{\Gamma}\right)^2} \tag{13}$$

Thus, we can see that the weight of the tube diameter measurement accuracy is 5 on the final evaluation of the friction factor. The next most influential term is the mass flow (Γ) term due to its squared appearance in Eq. (7). The thermal mass flow meter has a certified accuracy of less than ±1%, but in the case of the pipette measuring system the term can be expanded:

$$\left(\frac{2e_\Gamma}{\Gamma}\right)^2 = \left(\frac{2e_{u_{\text{pip}}}}{u_{\text{pip}}}\right)^2 + \left(\frac{4e_{D_{\text{pip}}}}{D_{\text{pip}}}\right)^2 + \left(\frac{2e_{T_{\text{pip}}}}{T_{\text{pip}}}\right)^2 + \left(\frac{2e_{P_{\text{out}}}}{P_{\text{out}}}\right)^2 \tag{14}$$

where the terms subscripted pip refer respectively to the meniscus velocity, diameter and temperature in the pipette. The error on the density, ρ, depends on the accuracy of the temperature (absolute scale) and pressure measurements. The pressure in the pipette is assumed equal to the channel outlet, i.e. ambient. Thus, with this system of measurement, it is apparent why a certain level of mass flow is desired: for extremely low flow rates, effects like meniscus evaporation and perhaps film reflux become too incumbent on the precision of the meniscus velocity u_{pip} and the pipette diameter D_{pip}, though it is impossible to determine exactly how much. These are parameters that furthermore weigh distinctly in the overall accuracy, so that the dispersion of data that was observed for small diameters (and thus small flow rates) with this method, is explained.

With the specified (or standard) uncertainties of the several parameters, a total experimental accuracy on the measured friction factor is obtained, for example for the 30 μm test section at $Re = 10$, of ±19% with the mass flow meter implemented, and of ±27% with the pipette. This means that the minimum Knudsen number that can be evidenced in our experiments, assuming a first-order slip model, will be (Eq. (12)) 17.5×10^{-3} for the former system, and only 25×10^{-3} for the pipette-measured mass flow method. From Table 1 it is clear that we operate below this range, so that any slip-flow effects at our conditions, would be hidden within the experimental error band. This is also the case for the larger diameters, where the Knudsen values are even lower.

4. Results and discussion

The results are presented in Figs. 6–9 in the form of *Po* vs. *Re* plots; one for each of the diameters tested. First of all, comparing the two Eqs. (4) and (6) for the friction factor, valid for isothermal or adiabatic conditions respectively, it should be stated that in (continuum) microscale *gas* flow, viscous heating effects are negligible. This means that in ambient conditions both isothermal and adiabatic approximations are valid. The difference in value between

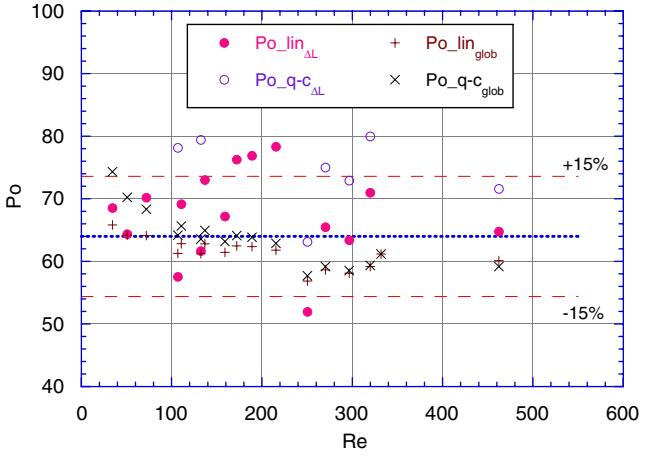

Fig. 6. Poiseuille vs. Reynolds number ($D = 254$ μm), linearized and quasi-compressible, local (ΔL) and global (glob) values.

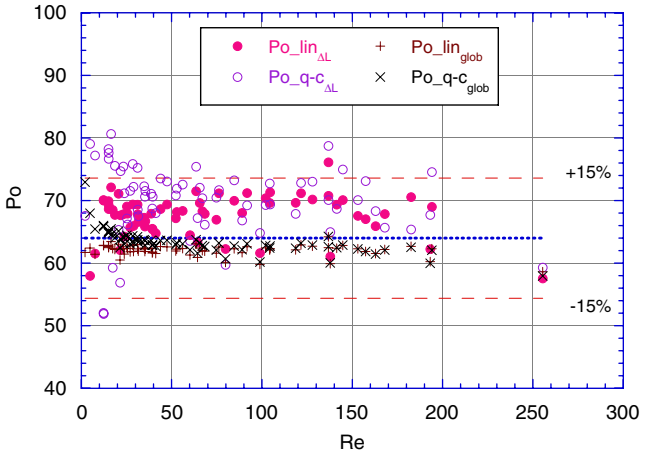

Fig. 7. Poiseuille vs. Reynolds number ($D = 101$ μm), linearized and quasi-compressible, local (ΔL) and global (glob) values.

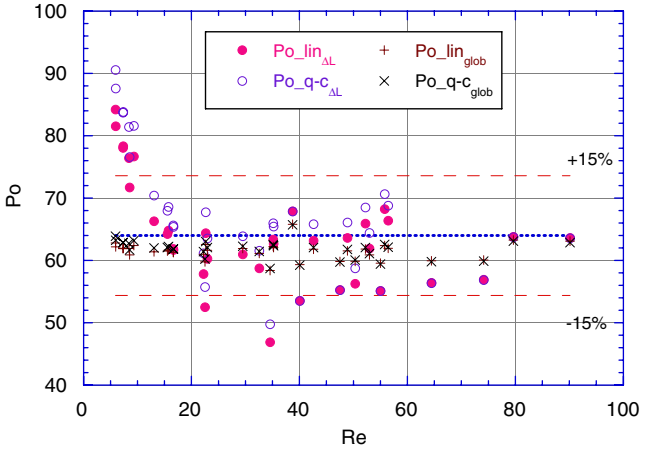

Fig. 8. Poiseuille vs. Reynolds number ($D = 50$ μm), linearized and quasi-compressible, local (ΔL) and global (glob) values.

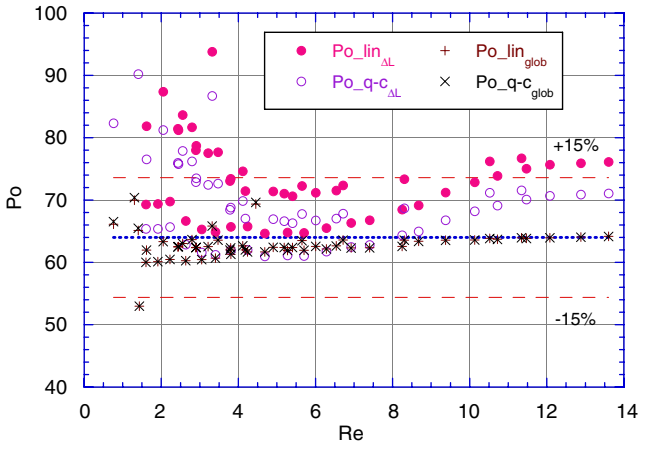

Fig. 9. Poiseuille vs. Reynolds number ($D = 30$ μm), linearized and quasi-compressible, local (ΔL) and global (glob) values.

the two never reached 1% in these experiments, both in global as in local characterization. For reasons of clarity therefore, only the isothermal approximation is presented in the graphs (as the quasi-compressible expression), but the adiabatic values can be considered as overlaying.

The results for the largest capillary, $D = 254$ μm, are presented in Fig. 6. Transition to turbulence was not reached because of the upper limit of functionality of the pipette volume flow measuring system. There is a large amount of dispersion in the data, especially in the differential (ΔL) analysis. This is due to the relatively short tubes studied and the small difference in length between the two sections: only 60 diameters (see Table 1). Coupled with the large diameter, this resulted in measured pressure (difference) values that were extremely small and therefore subject to high relative uncertainties. At low flow rates this effect is accentuated. This shows that the difference in length between the two tubes, though it should be as small as possible for an accurate derivation of the pressure slope (see Fig. 2), should also not be so little that measurement inaccuracy and flow oscillations interfere notably.

The global analysis allows for a less precarious measurement, although it omits elimination of concentrated pressure losses, and is a lot more stable, so that we can conclude that incompressible flow ($Po = 64$) is approximated quite nearly up to a Reynolds number of about 500, with a corresponding pressure ratio of 2.15 between inlet and outlet, and an outlet Mach number of 0.22.

This is probably also related to the relatively higher inaccuracy of the absolute pressure transducers (especially at low pressures) compared to the differential manometer. The latter value can be used in Eq. (7), but Eq. (4) requires absolute pressure measurements.

In Fig. 7 the analysis of experiments on the 101 μm diameter tube is represented. Data points are well-situated around the reference line of the theoretical Poiseuille number for incompressible flow, 64. The linearized and quasi-compressible analyses give similar results demonstrating behaviour that is equivalent to incompressible flow. It can be seen that the linear approximation of the *global* friction factor (Po_lin_{glob}) is equally as consistent as the more accurate correlations Eqs. (4) and (6), also at higher values of the Reynolds number and therefore larger pressure ratios. The maximum Mach number was 0.23 at the channel outlet ($Re = 255$). Data dispersion is more pronounced in the *differential* analysis, due to the summing of measurement errors for the two lengths of capillary. The *global* elaboration is consistent with incompressible theory, with a very slight bias to lower *Po* values.

In the case of the 50 μm diameter micropipe (see Fig. 8), it is remarkable to note that even at quite large pressure ratios ($R_P = 9.2$, $Re = 75$, $Ma = 0.19$), therefore where the density variation in the tube is considerable, the *global* linearized determination (Po_lin_{glob}) still follows the more elaborate approximation of compressible flow behaviour ($Po\_q\text{-}c_{glob}$) almost perfectly. The differential evaluations maintain a larger dispersion, but also converge closely around the reference line, which, it is remembered, is valid for completely incompressible flow.

The smallest channel in this study has a diameter of 30 μm. The elaborated data for the various interpretations of the Poiseuille number are shown in Fig. 9. It is clear then, that compressibility effects are negligible as regards the fluid-dynamic behaviour on the scale of a long tube (where the L/D value is very large), because the *global* correlations (linearized and quasi-compressible) give perfectly coherent results with the incompressible solution for tubes, $fRe = 64$.

The *local* Poiseuille number however, apart from the increased uncertainty of mass flow measurements at low Reynolds numbers, demonstrates a slight increment with respect to its global counterpart, especially in the linear approximation. This would go to indicate that the pressure derivative along the axis is steeper in the region after the inlet than the linear interpolation of Fig. 2. This would indicate a profile there that is convex rather than concave, which might reflect extended inlet effects, which are then "laminarized" along the channel. The latter must also be the phenomenon that explains somewhat the absence of any appreciable effects of compressibility. These effects – in particular, increased friction due to density-change-induced acceleration – were expected to become relevant when high head loss takes place over short distances like in microchannels. Instead we find that the layers in the flow are not affected by the change in fluid velocity profile in an irreversible way, in other words with very little extra entropy gain. This is confirmed by the measured temperature rise which was always extremely reduced, and the fact that both the isothermal and adiabatic equations for the friction factor (Eqs. (4) and (6)) yielded always almost equal solutions. This also implies that no "anomalous" energy conversion takes place with respect to incompressible flow in the low sub-sonic region ($Ma < 0.3$). Thus it can be stated that the pressure profile as sketched in Fig. 1, is quite exaggerated, and that there is certainly therefore such a thing as a fully developed "self-similar" velocity profile (Van der Berg et al., 1993a), which – although it is changed in

magnitude along the direction of flow – yields locally stable frictional resistance. This is what is after all defined in the Reynolds number, where the bulk mass flow compensates for both the density and the velocity:

$$Re = \frac{\rho UD}{\mu} = \frac{4\Gamma}{\pi\mu D} \tag{15}$$

for circular cross-sections. Therefore, within the range of accuracy, it is licit to confirm not only the validity of the "quasi-compressible" equations for the friction factor, but also of the actual incompressible description given in Eq. (7). And that the value of this factor is inversely proportional to the Reynolds number, with Poiseuille constant equal to 64.

5. Conclusions

An experimental investigation has taken place to determine the effects of compressibility for helium flowing through fused silica microtubes. The high frictional head loss per unit length in microscale channels was expected to cause an increase in the resistance to flow with respect to incompressible fluids, due to density-change-induced acceleration. This would cause a constantly developing velocity profile and therefore altering viscous deformation, as has been explained in the article. The drastic density change along the channel was expected to manifest literally the arising of "compressibility" effects. Experimental determination of local and global friction factors however, have mitigated this expectation. Pressure and mass flow measurements were elaborated to yield friction factors based on a linearized and a "quasi-compressible" pressure profile along the channel, and have exposed a behaviour which *quantitatively* in any case, and for relatively long channels, is indistinguishable from incompressible (microscale) flow. This means that the friction factor taken over an appreciable length of tube is inversely proportional to the Reynolds number only, with Poiseuille constant equal to 64, for the range of flow investigated. This range of validity can be expressed in terms of experimental parameters by considering the following limitation, based on Eq. (7):

$$f(1+U_f) \geqslant \frac{\pi^2\rho(R_P-1)P_{\text{out}}D^5}{8\Gamma^2 L} \tag{16}$$

where the pressure drop over the capillary ΔP is rewritten in terms of the pressure ratio, R_P, and the experimental uncertainty U_f defines the range of accuracy of the equality. Inserting the incompressible solution for $f\,(64/Re)$, yields the limit of the pressure ratio that allows such an approximation for compressible fluids:

$$R_P \leqslant 1 + \frac{128(1+U_f)\mu L\Gamma}{\pi D^4 \rho P_{\text{out}}} \tag{17}$$

Furthermore, the effects of inlet and outlet can be considered of minor importance. A tube cutting method was utilised to eliminate these but this objective was evidently nullified by the extremely limited magnitude of these effects. The increase in measurement uncertainty with this method therefore proved more distorting to measurements than the concentrated losses included in the global analyses. The latter type of evaluation consistently yielded a tight adherence to the theoretical Poiseuille number, so that the concentrated losses can be deemed insignificant within the limits of experimental detection.

Acknowledgements

The invaluable technical support of Michele Sica and the helpfulness of Dr. Emanuele Serra are gratefully acknowledged. This publication was made possible in part by the EU, FP6 project HMTMIC, RTN Contract HPRN-CT-2002-00204.

References

Asako, Y., Nakayama, K., Shinozuka, T., 2005. Effect of compressibility on gaseous flows in a micro-tube. Int. J. Heat Mass Transfer 48, 4985–4994.

Beskok, A., George, E.K., William, T., 1996. Rarefaction and compressibility effects in gas microflows. ASME J. Fluid Eng. 118, 448–456.

Celata, G.P., 2004. Single-phase heat transfer and fluid flow in micropipes. Heat Transfer Eng. 25 (3), 13–22.

Celata, G.P., Cumo, M., McPhail, S., Zummo, G., 2006. Characterization of fluid dynamic behaviour and channel wall effects in microtube. Int. J. Heat Fluid Flow 27, 135–143.

Choquette, S.F., Faghri, M., Kenyon, E.J., Sunden, B., 1996. Compressible fluid flow in micron sized channels, HTD-Vol. 327. In: Proceedings of the National Heat Transfer Conference, vol. 5, pp. 25–32.

Ettre, L.S., Hinshaw, J.V., 1993. Basic Relationships of Gas Chromatography. Advanstar Communications.

Fox, R.W., McDonald, A.T., 1994. Introduction to Fluid Mechanics, fourth ed. John Wiley & Sons.

Guo, Z.Y., Wu, X.B., 1997. Compressibility effect on the gas flow and heat transfer in a microtube. Int. J. Heat Mass Transfer 40, 3251–3254.

Guo, Z.Y., Wu, X.B., 1998. Further study on compressibility effect on the gas flow and heat transfer in a microtube. Microscale Thermophys. Eng. 2, 111–120.

Harley, J., Huang, Y., Bau, H., Zemel, J., 1995. Gas flow in microchannel. J. Fluid Mech. 284, 257–274.

Kohl, M.J., Abdel-Khalik, S.I., Jeter, S.M., Sadowski, D.L., 2005. An experimental investigation of microchannel flow with internal pressure measurements. Int. J. Heat Mass Transfer 48, 1518–1533.

Morini, G.L., Lorenzini, M., Spiga, M., 2004. A criterion for the experimental validation of the slip-flow models for incompressible rarefied gases through microchannels. In: Proceedings of the 2nd International Conference on Microchannels and Minichannels, pp. 351–358.

Perry, R.H., Green, D.W., 1999. Perry's Chemical Engineers' Handbook. McGraw-Hill, p. 6–92.

Turner, S.E., Lam, L.C., Faghri, M., Gregory, O.J., 2004. Experimental investigation of gas flow in microchannels. J. Heat Transfer 126 (5), 753–763.

Van der Berg, R.H., Seldam, C.A., Van der Gulik, P.S., 1993a. Compressible laminar flow in a capillary. J. Fluid Mech. 246, 1020.

Van der Berg, R.H., Seldam, C.A., Van der Gulik, P.S., 1993b. Thermal effects in compressible viscous flow in a capillary. Int. J. Thermophys. 14, 865–892.